Molecular Therapy
Nucleic Acids
Original Article

A Simplified System to Express Circularized Inhibitors of miRNA for Stable and Potent Suppression of miRNA Functions

Yi Shu,[1,2] Ke Wu,[2,3,4] Zongyue Zeng,[2,3,4] Shifeng Huang,[2,3,4] Xiaojuan Ji,[1,2] Chengfu Yuan,[2,5] Linghuan Zhang,[1,2] Wei Liu,[2,3,4] Bo Huang,[2,3,4,6] Yixiao Feng,[2,3,4] Bo Zhang,[2,7,8] Zhengyu Dai,[2,9] Yi Shen,[2,10] Wenping Luo,[2,3,4] Xi Wang,[2,3,4] Bo Liu,[2,3,4] Yan Lei,[2,3,4] Zhenyu Ye,[2,11] Ling Zhao,[2,3,4] Daigui Cao,[2,3,4] Lijuan Yang,[2,7,8] Xian Chen,[2,12] Hue H. Luu,[2] Russell R. Reid,[2,13] Jennifer Moriatis Wolf,[2] Michael J. Lee,[2] and Tong-Chuan He[1,2]

[1]Stem Cell Biology and Therapy Laboratory, Ministry of Education Key Laboratory of Child Development and Disorders, The Children's Hospital of Chongqing Medical University, Chongqing 400014, China; [2]Molecular Oncology Laboratory, Department of Orthopaedic Surgery and Rehabilitation Medicine, The University of Chicago Medical Center, Chicago, IL 60637, USA; [3]Ministry of Education Key Laboratory of Diagnostic Medicine, School of Laboratory Medicine, The Affiliated Hospitals of Chongqing Medical University, Chongqing 400016, China; [4]Department of Pharmacology, School of Pharmacy, Chongqing Medical University, Chongqing 400046, China; [5]Department of Biochemistry and Molecular Biology, China Three Gorges University School of Medicine, Yichang 443002, China; [6]Department of Clinical Laboratory Medicine, The Second Affiliated Hospital of Nanchang University, Nanchang 330006, China; [7]Key Laboratory of Orthopaedic Surgery of Gansu Province, First and Second Hospitals of Lanzhou University, Lanzhou 730030, China; [8]Departments of Orthopaedic Surgery and Obstetrics and Gynecology, First and Second Hospitals of Lanzhou University, Lanzhou 730030, China; [9]Department of Orthopaedic Surgery, Chongqing Hospital of Traditional Chinese Medicine, Chongqing 400021, China; [10]Department of Orthopaedic Surgery, Xiangya Second Hospital of Central South University, Changsha 410011, China; [11]Department of General Surgery, the Second Affiliated Hospital of Soochow University, Suzhou 215004, China; [12]Department of Clinical Laboratory Medicine, Affiliated Hospital of Qingdao University, Qingdao 266061, China; [13]Department of Surgery, Section of Plastic Surgery, The University of Chicago Medical Center, Chicago, IL 60637, USA

MicroRNAs (miRNAs) are an evolutionarily conserved class of small regulatory noncoding RNAs, binding to complementary target mRNAs and resulting in mRNA translational inhibition or degradation, and they play an important role in regulating many aspects of physiologic and pathologic processes in mammalian cells. Thus, efficient manipulations of miRNA functions may be exploited as promising therapeutics for human diseases. Two commonly used strategies to inhibit miRNA functions include direct transfection of chemically synthesized miRNA inhibitors and delivery of a gene vector that instructs intracellular transcription of miRNA inhibitors. While most miRNA inhibitors are based on antisense molecules to bind and sequester miRNAs from their natural targets, it is challenging to achieve effective and stable miRNA inhibition. Here we develop a user-friendly system to express circular inhibitors of miRNA (CimiRs) by exploiting the noncanonical head-to-tail backsplicing mechanism for generating endogenous circular RNA sponges. In our proof-of-principle experiments, we demonstrate that the circular forms of the hsa-miR223-binding site of human β-arrestin1 (ARRB1) 3′ UTR sponge RNA (BUTR), the bulged anti-miR223 (cirBulg223) and bulged anti-miR21 (cirBulg21), exhibit more potent suppression of miRNA functions than their linear counterparts. Therefore, the engineered CimiR expression system should be a valuable tool to target miRNAs for basic and translational research.

INTRODUCTION

MicroRNAs (miRNAs) are an evolutionarily conserved class of small regulatory noncoding RNA molecules consisting of 18–25 partially complemented double-stranded nucleotides, and they play a central role in regulating cell differentiation, proliferation, and survival by binding to complementary target mRNAs, resulting in mRNA translational inhibition or degradation.[1–5] With the discovery of abundant expression of miRNAs in many organisms, these small noncoding RNAs catapulted onto the stage of posttranscriptional gene regulation nearly two decades ago.[2] In humans, it has been estimated that over 2,000 miRNAs are expressed, and more than 60% of the protein-coding genes contain at least one conserved miRNA-binding site.[6] Emerging evidence indicates that miRNAs are involved in almost all known physiologic and pathologic processes.[4,5,7,8]

Originally derived from longer primary miRNA transcripts, approximately 22-nt-long double-stranded miRNAs are formed by

Received 22 July 2018; accepted 26 September 2018;
https://doi.org/10.1016/j.omtn.2018.09.025.

Correspondence: Tong-Chuan He, MD, PhD, Molecular Oncology Laboratory, Department of Orthopaedic Surgery and Rehabilitation Medicine, The University of Chicago Medical Center, 5841 South Maryland Avenue, MC 3079, Chicago, IL 60637, USA.
E-mail: tche@uchicago.edu
Correspondence: Ke Wu, MD, PhD, Department of Pharmacology, School of Pharmacy, Chongqing Medical University, Chongqing 400046, China.
E-mail: wukecqmu@163.com

successive processing steps, after which one strand is incorporated into the RNA-induced silencing complex (RISC).[1–5] Mechanistically, miRNA guides RISC to complementary mRNA target sequences mainly located in 3′ UTRs. In humans, the sequence complementarity between mRNA and miRNA is usually imperfect, but base pairing involving the seed region, nucleotides 2–7 of the miRNA as counted from the 5′ end, is particularly important for target recognition, and in many cases it is sufficient to facilitate miRNA-directed gene silencing.[9,10] Such partial mRNA:miRNA complementarity promotes mRNA deadenylation or translational repression, whereas near-perfect complementarity promotes mRNA cleavage at a position opposite to nucleotides 10–11 of the miRNA.[1–5] Some miRNAs are expressed in virtually all cell types, whereas others are highly tissue specific, with a distinct function in a particular cell type or organ.[1–5]

While miRNAs can regulate most protein-coding genes, miRNAs are targeted by many regulatory RNA species as several classes of noncoding RNA molecules contain miRNA-binding sites. Such miRNA sponges bind miRNAs and competitively sequester them from their natural targets.[10] Endogenous miRNA sponges or competing endogenous RNAs (ceRNAs), which include endogenously transcribed pseudogenes, long noncoding RNAs, and circular RNAs (circRNAs), can act to buffer the activity of miRNAs on physiologically relevant targets.[10] Thus, efficient modulations of miRNAs may be exploited as promising therapeutics for cancer treatment and other human diseases.

For the past decades, significant efforts have been devoted to the development of miRNA inhibitors, commonly referred to as antimiRs, antagomiRs, AMOs (anti-miRNA antisense oligonucleotides), miRNA sponges, or miRNA decoys, most of which are usually based on antisense molecules to bind and sequester miRNAs from their natural targets.[4,9,10] In general, miRNA inhibition can be accomplished by two approaches: direct transfection of chemically synthesized inhibitors[11,12] or delivery of a vector that encodes intracellular transcription of RNA inhibitors.[9,10] Although synthetic miRNA inhibitors are suitable for many *in vitro* experimental applications, the *in vivo* utilities of synthetic miRNA inhibitors are usually limited due to poor delivery efficiency and stability. The naturally occurring miRNA sponges have provided inspiration for engineering of gene vector-encoded sponges as potent miRNA inhibitors *in vivo*, and the expression of custom-designed sponges offers new means of controlling miRNAs for therapeutic regulation of gene expression.[9,10] Nonetheless, it remains technically challenging to express effective and potent miRNA inhibitors *in vitro* and *in vivo*.

Recent studies identified noncoding circRNA molecules that may serve as potent endogenous sponges.[13–18] Such circular transcripts are primarily derived from noncanonical head-to-tail splicing events through a backsplicing mechanism.[13–16] It has been reported that circular conformation renders these RNA molecules several advantages, including effective miRNA sequestration, increased stability, more resistance to exonucleolytic RNA degradation, and resistance to miRNA-mediated noncleavage destabilization with susceptibility to miRNA-mediated cleavage.[9,10,19]

Inspired by the underlying mechanism for the production of endogenous circRNA sponges, here we develop a user-friendly system to express the circular inhibitors of miRNA (CimiRs) by taking advantage of the noncanonical head-to-tail backsplicing mechanism. The splicing sites are brought to a close proximity by two 100-bp inverted repeat (IR) sequences. In our proof-of-principle experiments, we demonstrate that the circular forms of the miR223-binding site of human β-arrestin1 (ARRB1) 3′ UTR sponge RNA (BUTR), the bulged anti-miR223 (cirBulg223) and bulged anti-miR21 (cirBulg21), exhibit more potent suppression of the miRNA functions than their linear counterparts. Therefore, the engineered CimiR expression system should be a valuable tool to target miRNAs for basic and translational research.

RESULTS

Development of a Simple and Effective circRNA Expression System

As previously reported, circRNA can be generated in a *cis* backsplicing process.[13–15,17,18,20] To effectively express circularized RNA molecules, we engineered a retroviral vector, namely pSEBR-CimiR, which contains the following components: a 100-bp IR derived from mouse Rosa26 genomic DNA, a splicing branch site, a polypyrimidine track, a cloning linker, a splicing donor site, a 20-bp random sequence, and the IR sequence in inverse orientation (Figure 1A).

For generating properly controlled linear RNA products, we also engineered the pSEBR-LimiR vector, which contains the same components as that of pSEBR-CimiR except the 5′ end IR sequence, the splicing branch site, and the polypyrimidine track (Figure 1A).

The whole CimiR or LimiR cassette is driven by the human elongation factor 1α-HIV enhancer hybrid promoter (hEFH) promoter[21,22] (Figure 1B). The CimiR pre-mRNA transcripts can be processed through a *cis* backsplicing mechanism to yield the desired circularized antamiR (CimiR) molecules and splicing by-products (Figure 1C).

A Circularized Sponge RNA Derived from ARRB1 3′ UTR Effectively Antagonizes hsa-miR223-Mediated Repression of Target Gene Expression

As one of the proof-of-principle studies, we examined the anti-miR223 effect of a circular sponge RNA derived from the ARRB1 3′ UTR region (402 bp) containing a validated hsa-miR223-binding site (BUTR) (Figure 2A). We subcloned the BUTR into the pSEBR-CimiR and pSEBR-LimiR, yielding pSEBR-circular BUTR (cirBUTR) and pSEBR-linear BUTR (linBUTR), respectively. Transient transfection of these vectors into HEK293 cells was carried out, and semi-quantitative RT-PCR analysis confirmed the presence of cirBUTR in the pSEBR-cirBUTR-transfected cells, but not in the pSEBR-linBUTR-transfected cells, using the converging primers (Figure 2A), indicating that the *cis* backsplicing mechanism-based circRNA expression system was functional.

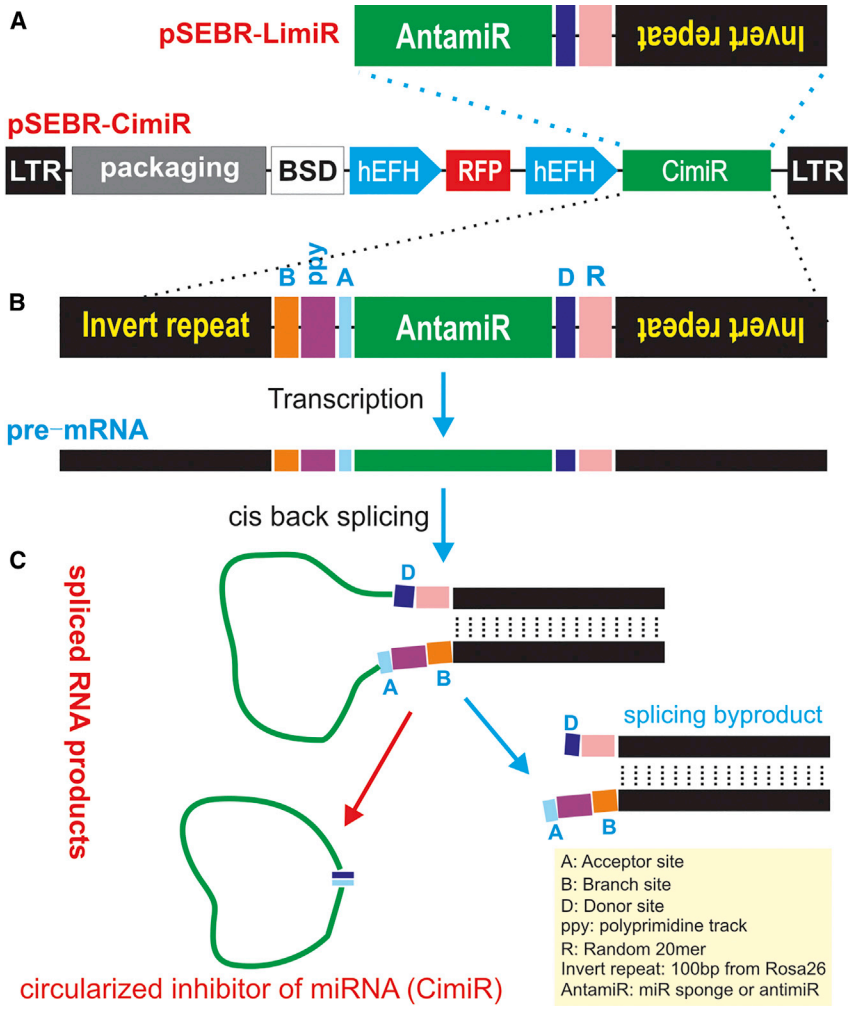

Figure 1. Schematic Representation of the CimiR System for Expressing the Circularized AntamiRNAs or miRNA Antagonists

(A and B) Overall structure (A) and the essential elements (B) of the CimiR system. Briefly, the consensus sequences of the RNA-splicing branch site (B) and polypyrimidine track (ppy) were constructed at the 5′ end of the antamiRNA locus, while the donor site sequence (D) and a 20-mer random sequence (R) were engineered at the 3′ end of AntamiR, which were flanked by the 100-bp inverted repeat sequence derived from mouse Rosa26 genomic sequence. (C) Formation of a circularized antamiR (or CimiR). Upon transcription driven by the hEFH promoter, the antamiR-containing pre-mRNA is processed through *cis* backsplicing mechanism to yield a circularized antamiR (CimiR) and a splicing by-product. The expression system was constructed on the basis of retroviral vector pSEBR, which expresses blasticidin selection marker and RFP-tracking marker. The same CimiR expression cassette was constructed in an adenoviral shuttle vector pAdTrace-CimiR as well.

We first compared the transcript stability of the cirBUTR and linBUTR. Both pSEBR-cirBUTR and pSEBR-linBUTR were transfected into HEK293 cells and treated with actinomycin D for 0, 3, and 8 hr. Total RNA was isolated and reverse transcribed for assessing the expression of cirBUTR and linBUTR, as well as the RFP expression level in the transfected cells. Our results indicated that cirBUTR expression level did not decrease but rather increased at 8 hr after actinomycin D treatment, while linBUTR expression decreased significantly after actinomycin D treatment (Figure 2B). It is noteworthy that the initial expression levels of cirBUTR and linBUTR were rather comparable. Quantitatively, the expression of cirBUTR was about six times more stable than Gapdh, while the expression of linBUTR was approximately only 10% of GAPDH mRNA at 8 hr after actinomycin D treatment (Figure 2B). These results suggest that the cirBUTR may act as a more powerful miRNA sponge to antagonize its target miRNA.

To further confirm the functionality of the circular sponge RNA cirBUTR, we infected the human T cell acute lymphoblastic leukemia (T-ALL) cell lines Jurkat and CCRF-CEM with the retrovirus expressing linBUTR or cirBUTR or with the seed sequence scrambled circRNA (SCR) expression control vector, and we tested the efficiency of linBUTR and cirBUTR to antagonize oncogenic miR (oncomiR)-miR223 fucntions. We have recently demonstrated that oncomiR miR223 is highly expressed in T-ALL cells and clinical samples (data not shown). Our qPCR analysis of three well-characterized miR223 target genes indicated that exogenous expression of cirBUTR effectively reversed the expression of ARRB1, FBXW7, and RHOB, while linBUTR expression marginally increased the expression of these target genes in Jurkat cells (Figure 2C). Similar trends were observed in CCRF-CEM cells as cirBUTR effectively increased the expression of ARRB1 and FBXW7, while linBUTR only increased the expression of ARRB1, and neither cirBUTR nor linBUTR affected the expression of RHOB (Figure 2D). Collectively, the above results indicate that the circular sponge RNA is seemingly more stable and possesses more potent antagonistic effects on miRNAs.

A Circularized Bulged Anti-miR223 Effectively Reverses hsa-miR223-Mediated Repression of Target Gene Expression and Induces Apoptosis in Human T-ALL Cells

To test whether the CimiR system can be exploited to express anti-miRs and achieve desirable miRNA antagonism, we engineered a tandem of miR223 sponge sequences, each of which was imperfectly matched to the mature hsa-miR223 sequence and separated by a 6-mer spacer as described (Figure 3A, a).[23–25] The circular and linear bulged miR223 sponges, along with the seed sequence SCR control fragments, were constructed (Figure 3A, b). We also constructed

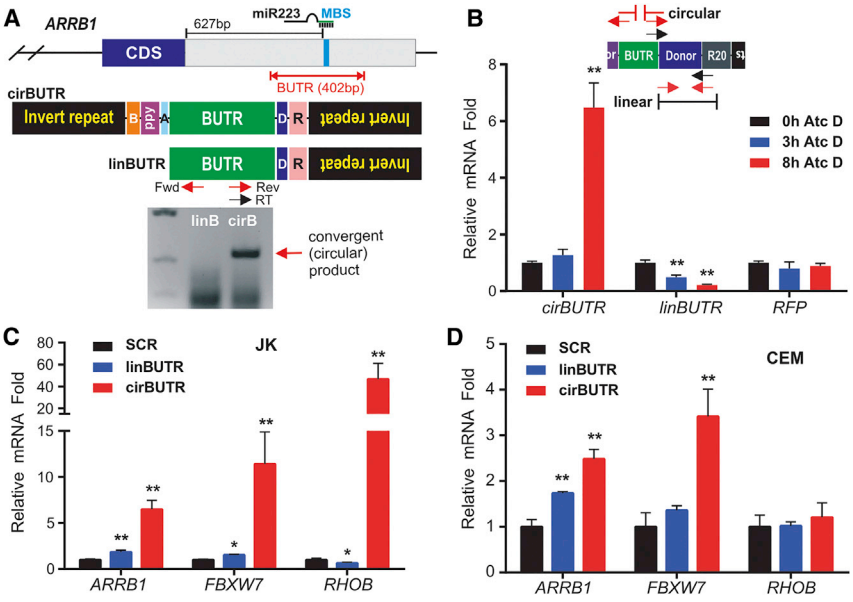

Figure 2. Efficient Antagonization of hsa-miR223 with the Circularized ARRB1-Derived RNA Sponge in T-ALL Cell Lines

(A) Schematic representation depicting hsa-miR223-binding site (MBS) at the 3′ end UTR (or BUTR) of human β-Arrestin1 (ARBB1). A 402-bp fragment containing MBS was PCR amplified and subcloned into the CimiR system, resulting in cirBUTR. Its linear counterpart linBUTR was also engineered as a control. Upon transfection into HEK293 cells, a specific circular product was readily detected by RT-PCR in the cirBUTR transfection group (indicated by the arrow), but not in the linBUTR group. (B) The circularized RNA sponge is more stable than the linear transcript. HEK293 cells were transfected with cirBUTR or linBUTR plasmid DNA and treated with actinomycin D for the indicated time, and total RNA was isolated and subjected to qRT-PCR analysis of the abundance of linear and circular forms of BUTR transcripts, while RFP mRNA was used as an exogenous transcript control. **$p < 0.01$. (C and D) Effective reversal of the expression of hsa-miR223-targeted genes by cirBUTR in T-ALL lines. The T-ALL cell lines Jurkat (C) and CCRF-CEM (D) were infected with the retrovirus stably expressing linBUTR, cirBUTR, or the seed sequence scrambled circRNA (SCR). The expression of miR223-targeted genes, such as *ARRB1*, *FBXW7*, and *RHOB*, was assessed by qPCR analysis. GAPDH was used as an internal control. *$p < 0.05$, **$p < 0.01$.

the miR223 overexpression vector, and we demonstrated it was highly expressed in transiently transfected HEK293 cells (Figure 3B, a). Furthermore, we showed that the exogenous expression of miR223 in HEK293 cells was not affected by the presence of linear miR223 sponge expression vector (linBulg223) or circular miR223 sponge expression vector (cirBulg223) (Figure 3B, b).

Our qPCR results indicated almost all six of the validated miR223 target genes were downregulated in HEK293-miR223 cells compared with the mock cells (Figure 3C). However, overexpression of circular miR223 sponge cirBulg223 significantly reversed the expression of five of the six tested target genes ($p < 0.01$) (Figure 3C). To a much lesser extent, expression of linBulg223 was shown to reverse the expression of 4 of the 6 target genes (Figure 3C).

We next analyzed whether the circular or linear miR223 sponge could effectively rescue the miR223-targeted reporter activity. We constructed the miR223 Gaussia luciferase reporter pNRGLuc-BUTR, and we transduced this reporter into HEK293-miR223 cells. Upon transduction of circular or linear miR223 sponge, we continuously monitored the GLuc activities, and we found that circular miR223 sponge significantly reversed the GLuc activities at 72–120 hr post-transfection (Figure 3D). Thus, the above results further demonstrate that the circular miR223 sponge cirBulg223 is much more potent in antagonizing miR223 functions than the linear linBulg223 sponge in HEK293 cells.

We further examined the biological outcomes of antagonizing miR223 with the circular and linear miR223 sponge in T-ALL cells. The miR223 is one of the well-established oncomiRs in T-ALL cells, and it is involved in the initiation and progression procession during the T cell leukemogenesis.[26,27] We previously found that a blockade of miR223 functions led to apoptosis in T-ALL cells. To test if the cirBulg223 would effectively antagonize miR223 in T-ALL cells, we infected the T-ALL cell lines Jurkat and CCRF-CEM with linBulg223, cirBulg223, or the seed sequence scrambled circRNA retroviral vectors. At 48 hr after infection, we examined the presence of cleaved caspase-3 by immunostaining. While no RFP+ cells were found undergoing apoptosis after infection with seed sequence scrambled circRNA retroviral vectors (Figure S1), most of the RFP+ cells, which expressed cirBulg223, stained positive for cleaved caspase-3 in both Jurkat (Figure 4A, a) and CCRF-CEM (Figure 4A, b) cells. Conversely, a smaller portion of the RFP+ cells that expressed linBulg223 stained positive with cleaved caspase-3 in both T-ALL lines (Figure 4A). Quantitatively, we found that, while linBulg223 expression led to only 60% of the RFP+ Jurkat cells undergoing apoptosis, cirBulg223 expression led to >90% RFP+ Jurkat cells undergoing apoptosis (Figure 4B). Interestingly, in the CCRF-CEM line, the apoptotic rate of linBulg223-expressing cells was approximately 20%, while cirBulg223-expressing cells exhibited about a 50% apoptosis rate (Figure 4B). We also carried out qPCR analysis of miR223 target genes, and we found that both miR223 sponges were able to rescue the expression for two of the three miR223 target genes in Jurkat and CCRF-CEM cell lines, although the circular miR223 sponge consistently outperformed the linear counterpart in both cell lines (Figure 4C, a and b). Taken together, our results strongly demonstrate that the circular anti-miR233 sponge is more potent than its linear counterpart in antagonizing miR223 functions.

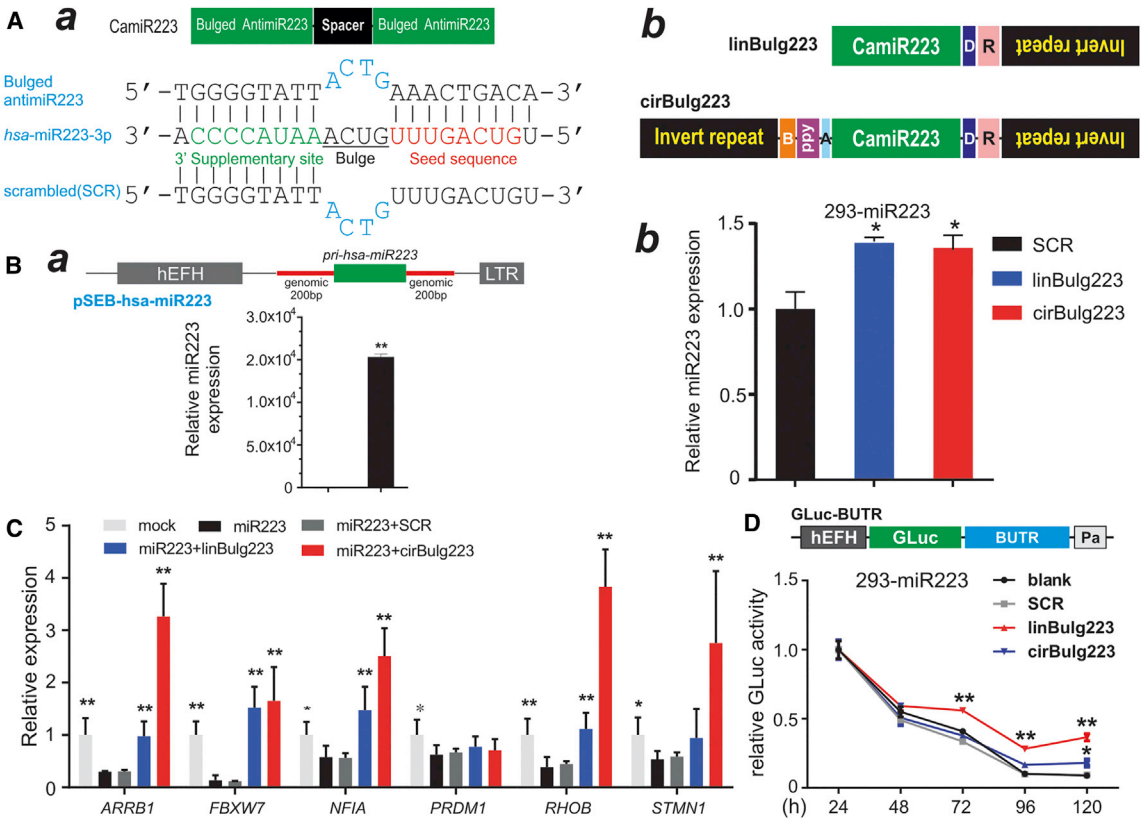

Figure 3. Restoration of the Expression of hsa-miR223-Targeted Genes with the Circular Bulged Anti-miR223

(A) Schematic representation of the designs of circular and linear bulged anti-miR223 constructs along with the seed sequence SCR. Bulged anti-miR223 (or CimiR223) was designed against hsa-miR223-3p as described (a).[23–25] Two copies of the CimiR223 were subcloned in the pSEBR-CimiR vector to generate the circular bulged anti-miR223 (cirBulg223) and the linear bugled anti-miR223 (linBulg223) (b). (B) Exogenous expression of hsa-miR223. A genomic DNA fragment containing the pri-hsa-miR223-coding region and 200 bp upstream and 200 bp downstream of the pri-hsa-miR223-coding region was PCR amplified and cloned into a retroviral vector, resulting in pSEB-hsa-miR223 (a). The expression of mature miR223 was detected by qPCR in the transfected HEK293 cells. Similarly, the expression of miR223 was not significantly affected by linBulg223 and cirBulg223 in the transiently transfected HEK293 cells (b). *$p < 0.05$. (C) Reversal of the expression of hsa-miR223-targeted genes with the circularized bulged anti-miR223. HEK293 cells were co-transfected with pSEB-hsa-miR223 or mock plasmid and linBulg223, cirBulg223, or scrambled control for 72 hr. The expression of miR223 target genes was assessed by qPCR. *$p < 0.05$, **$p < 0.01$ compared with miR223 versus mock or miR223 versus cirBulg223, linBulg223, or scrambled control. (D) Gaussia luciferase (GLuc) reporter assay. The miR223-expressing HEK293 cells (293-miR223) were co-transfected with pNRGLuc-BUTR reporter and linBulg223 expression vector, cirBulg223 expression vector, or SCR expression vector. GLuc activities were measured at the indicated time points. All assays were done in triplicate. GAPDH was used a reference gene. *$p < 0.05$, **$p < 0.01$.

A Circularized Bulged Anti-miR21 Effectively Inhibits the oncomiR Functions of hsa-miR21 and Attenuates Tumor Growth in a Xenograft Tumor Model of Human Breast Cancer

To further validate the general applicability of the CimiR system, we sought to construct a circular anti-miR21 sponge, and we tested its ability to antagonize the functions of oncomiR-miR21 in breast cancer cells.[28] Using a similar strategy as for designing the anti-miR223 sponge, we constructed the linear and circular antagonist miR21, linBulg21 and cirBulg21, and the seed sequence SCR expression vector. The retroviral vectors expressing linBulg21 and cirBulg21 were used to infect human breast cancer line MCF7 and SKBR3. We carried out qPCR analysis, and we found that the expression of known miR21 target genes BCL2, PDCD4, RASGRP, and TGFB1 was significantly upregulated while the expression of BTG2 and PTEN was downregulated in the cirBuld21-transduced MCF7, whereas some of the target genes were regulated by linBulg21 to a much lesser extent (Figure 5A). Similarly, the expression of cirBulg21 led to increased expression of BCL2, PDCD4, PTEN, RASGRP, and TGFB1 in SKBR3 cells, while linBulg21 expression exhibited similar changes but to a much lesser extent (Figure 5B). Western blotting analysis further confirmed that cirBulg21 expression led to the increased expression of BCL2 and PTEN in SKBR3 cells, while linBulg21 caused modest increases in the expression levels of BCL2 and PTEN (Figure 5C).

We further tested the effect of cirBulg21 expression on colony formation ability in breast cancer cells. Human breast cancer lines SKBR3 and MCF7 cells were infected with retroviral vectors

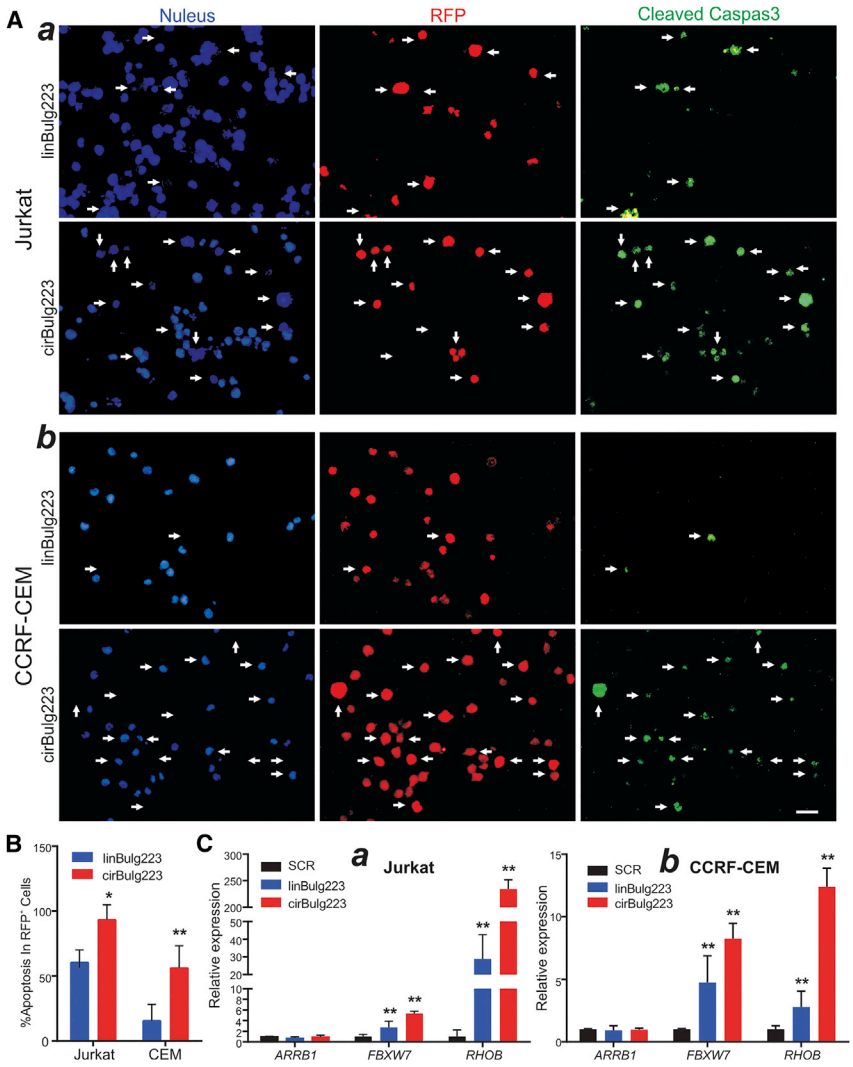

Figure 4. The Circular Bulged Anti-miR223 Effectively Antagonizes OncomiR miR223 and Induces Apoptosis in T-ALL Cells

(A) Human T-ALL cell lines Jurkat (JK) (a) and CCRF-CEM (CEM) (b) were infected with linBulg223 or cirBulg223 retrovirus, which also expresses RFP. At 48 hr after infection, the cells were fixed and subjected to immunostaining with the cleaved caspase-3 antibody. Cell nuclei were counterstained with DAPI. The cleaved caspase-3-positive cells and their RFP+ and DAPI+ counterparts are indicated by arrows. Assays were done in triplicate. Representative images are shown. Scale bar, 25 μm. (B) Quantitative analysis of apoptosis in the infected (RFP+) cells. *$p < 0.05$, **$p < 0.01$. (C) qPCR analysis of the expression of miR223 target genes in T-ALL cells. Jurkat (a) and CCRF-CEM (b) cells were infected with linBulg223, cirBulg223, or SCR control vectors. At 48 hr after infection, total RNA was isolated and subjected to qPCR analysis. **$p < 0.01$.

expressing cirBulg21, linBulg21, or the seed sequence SCR expression vector, and they were reseeded at two cell densities for a long-term culture. We found that the numbers of colonies formed in cirBulg21-transduced cells were significantly lower than the mock control in both SKBR3 and MCF7 cells, while the linBulg21-transduced cells formed modestly decreased numbers of colonies (Figure 5D). Moreover, cycle analysis also confirmed that cirBulg21 expression in SKBR3 cells led to an increase of cell numbers in G0/G1 phases and a decrease in M and G2/S phases, while linBulg21 expression led to a modest increase in G0/G1 phases and a decrease in M phase (Figure 5E).

To further test whether the circular anti-miR21 sponge expressed by the CimiR system would significantly affect tumor growth *in vivo*, the firefly luciferase-labeled SKBR3-FLuc cells were transduced with linBulg21, cirBulg21, or the seed sequence SCR expression vector, and they were implanted subcutaneously into the identical nude mice. Whole-body imaging analysis indicated that the cirBulg21-transduced SKBR3 cells grew more slowly than the linBulg21-transduced SKBR3 group or the mock control group at all of the examined time points (Figure 6A). Accordingly, at the endpoint, the average size of the retrieved tumor masses from the cirBulg21 group was much smaller than that from the linBulg21 group or scrambled control group (Figure 6B). Histologic evaluation further demonstrated that the tumor masses retrieved from the cirBulg21-transduced SKBR3 group exhibited extensive necrosis, accompanied by sparsely distributed proliferating tumor cells (Figure 6C). On the other hand, tumor masses retrieved from the linBulg21-transduced SKBR3 group or the scrambled control group contained highly proliferative cells (Figure 6C). Collectively, our *in vivo* results further demonstrate that the circular anti-miR21 sponge expressed by the CimiR system exhibits potent antagonistic effects on oncomiR-miR21 both *in vitro* and *in vivo*.

DISCUSSION

Stable and effective suppression of miRNAs is important for investigating miRNA biology and developing miRNA-based therapeutics. As an evolutionarily conserved class of small, regulatory noncoding RNA molecules, miRNAs play a central role in regulating cell differentiation, proliferation, and survival by binding to complementary target mRNAs, resulting in mRNA translational inhibition or degradation.[3,4] Conversely, miRNAs are also targeted by many regulatory RNA species, as several classes of noncoding RNA molecules contain miRNA-binding sites. Such miRNA sponges bind miRNAs and competitively sequester them from their natural targets.[10] Endogenous miRNA sponges or ceRNAs, which include endogenously transcribed pseudogenes, long noncoding RNAs, and circRNAs, can act to

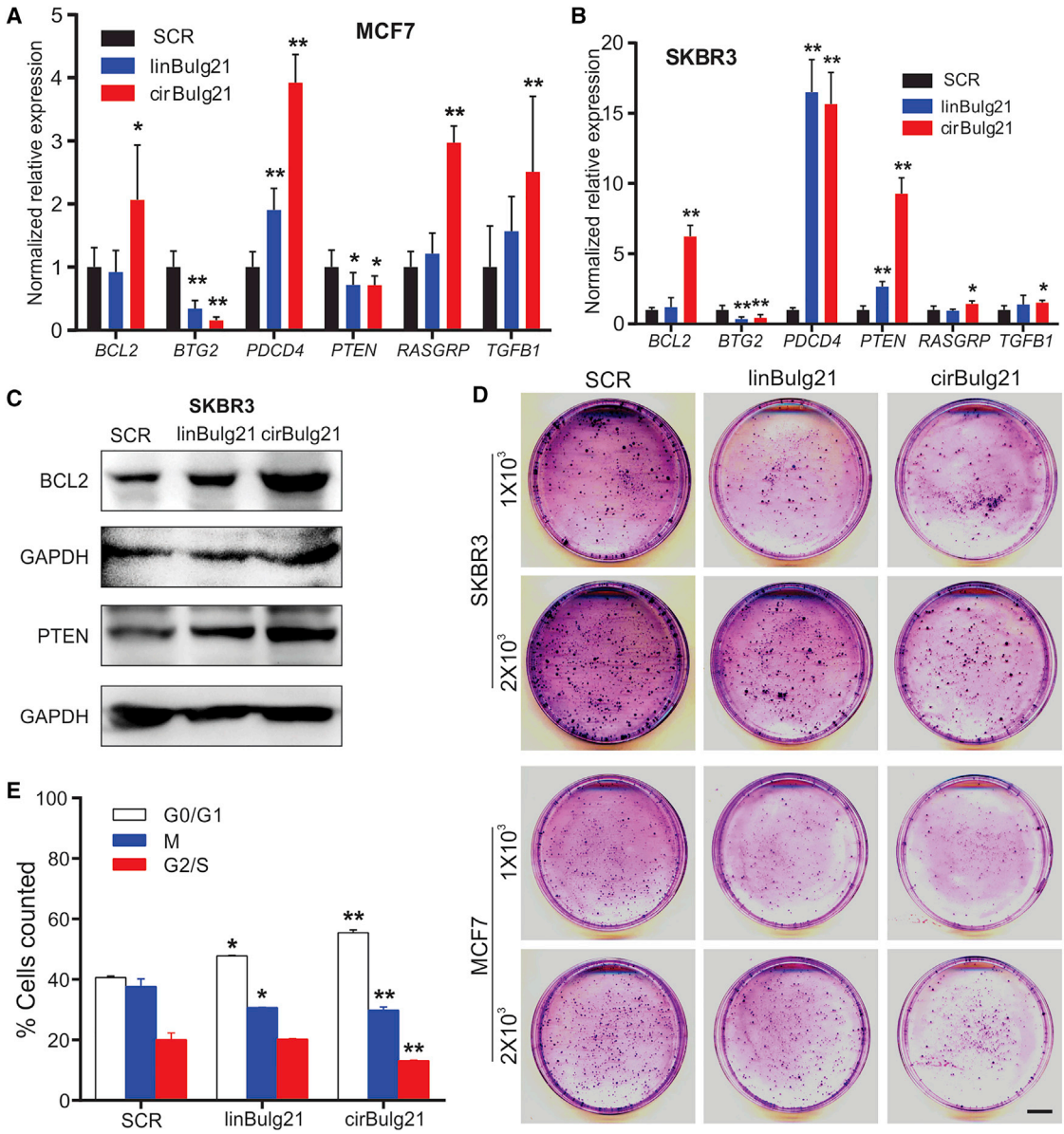

Figure 5. The Circular Bulged Anti-miR21 Effectively Inhibits hsa-miR21 Functions and Suppresses Cell Proliferation in Human Breast Cancer Cells

(A & B) qPCR analysis of the expression of hsa-miR21 target genes in breast cancer cells. The cirBulg21, linBulg21 vectors and miR21 seed sequence scrambled circRNA expression vector were constructed in the same fashion as that for antimiR223. Human breast cancer cell lines MCF7 (A) and SKBR3 (B) were infected with linBulg21, cirBulg21 or scrambled retroviral vector (SCR) for 72h. Total RNA was isolated and subjected to qPCR analysis using the qPCR primers for known miR21 target genes. All assays were done in triplicate. GAPDH was used a reference gene. "*" $p<0.05$; "**" $p<0.01$. (C) Western blotting analysis of hsa-miR21-regulated expression of BCL2 and PTEN in breast cancer cells. Human breast cancer cell line SKBR3 was infected with linBulg21, cirBulg21 or scrambled vector (SCR) for 72h. Total cell lysate was subjected to SDS-PAGE and Western blotting with BCL2 or PTEN antibody. GAPDH expression was used as internal/loading control. (D) Colony formation assay. SKBR3 and MCF7 cells were infected with linBulg21, cirBulg21 or scrambled retroviral vector (SCR) for 24h and subsequently seeded in 60mm cell culture dishes at 1X103 or 2X103 cells. Colonies were fixed and stained with crystal violet on day 12. Representative images are shown. (E) Cell cycle analysis. SKBR3 cells were infected with linBulg21, cirBulg21 or scrambled retroviral vector (mock) for 48h. Cells were collected and subjected to cell cycle analysis. Each assay condition was done in triplicate. "*" $p<0.05$, "**" $p<0.01$. Scale bar, 1 cm.

buffer the activity of miRNAs on physiologically relevant targets.[10] Thus, miRNAs have emerged as promising therapeutics for cancer treatment and other human diseases.

Even though loss of miRNA functions can be created in miRNA-knockout mouse models or mouse embryonic stem cells,[29,30] the generation of knockout mice is not straightforward for many miRNAs,

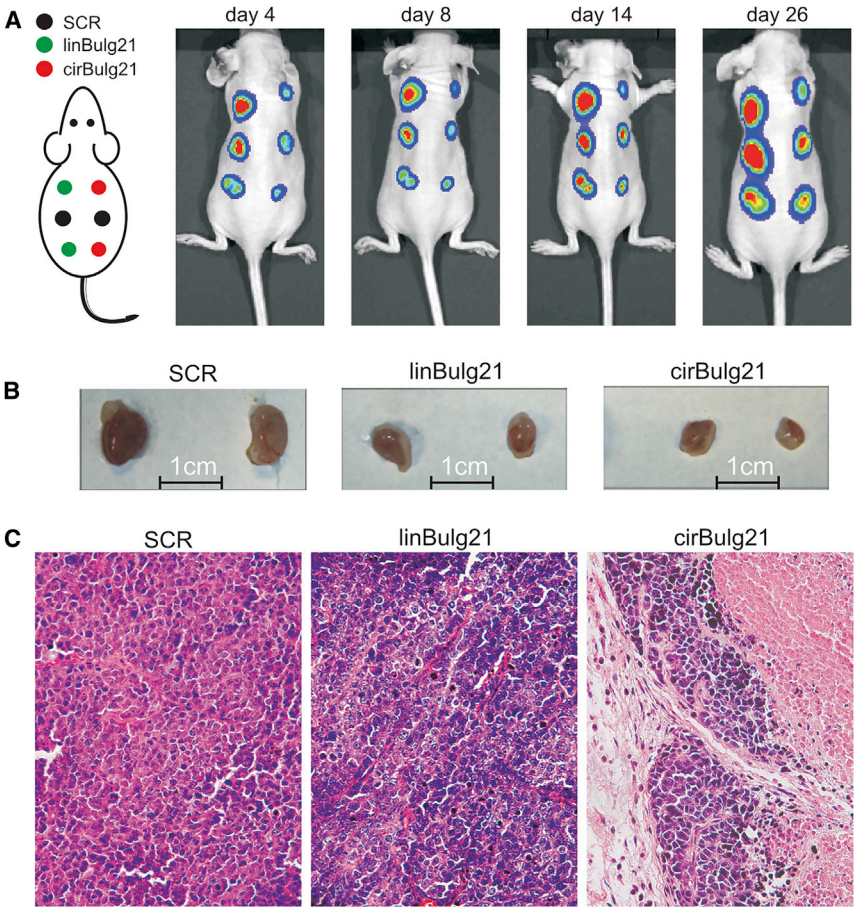

Figure 6. The Circular Bulged Anti-miR21 Inhibits Breast Cancer Growth *In Vivo*

SKBR3 cells were first stably labeled with firefly luciferase, and then infected with linBulg21, cirBulg21, or scrambled retroviral vector (mock) for 24 hr. The infected cells were collected and injected subcutaneously into athymic nude mice at 5×10^6 per injection (n = 5 mice). (A) Xenograft tumor growth was monitored by Xenogen IVIS bioluminescence imaging at the indicated time point. (B) The animals were sacrificed at 26 days after injection, and tumor masses were retrieved. Representative images are shown. (C) The retrieved tumor masses were fixed and subjected to paraffin embedment and sectioning, followed by H&E staining. Representative images are shown.

because some miRNAs originate from multiple distinct loci in the genome, and/or many miRNAs have seed family members that share mRNA targets. Furthermore, some miRNAs are located in an intron of a gene in which knockout of the miRNA sequence may confound gene expression.[9,10] Therefore, in many cases a knockout-based complete abrogation of miRNA activity in a particular cellular pathway is both laborious and technically challenging.[9,10] Rather, vector-encoded miRNA inhibitors provide an important alternative for suppressing a specific miRNA or families of miRNAs *in vitro* and/or in transgenic animals.

RNA molecules carrying target sequences for the desired miRNA constitute the most widely employed type of miRNA decoy-type inhibitors, which is based on the strategy to provide a surplus of miRNA recognition sites exposed in a structural RNA context with optimized affinity and specificity for the mature miRNA.[9,10] Such miRNA recognition site-containing decoy inhibitors range from short and simple antisense transcripts to structured scaffolds encompassing multiple miRNA-binding sites. It was originally thought that the miRNA target sites within sponges designed with full complementarity to the miRNA may achieve maximum targeting affinity. However, it was shown that the target sites were designed to give rise to an internal bulge opposite to nucleotides 10 and 11 of the miRNA, leading to enhanced inhibition potency.[23,31] Nonetheless, since a seed match is sufficient to facilitate miRNA target recognition, a single sponge can inhibit members of a whole miRNA family. The overall complementarity still governs the affinity between the miRNA and the target site, which leads to differential inhibition efficiency among the miRNAs in the family.[9,10] In our studies, both miR223 and miR21 inhibitors contained internal bulge nucleotide to ensure inhibition potency.

A high stability of miRNA inhibitors is essential to achieve effective suppression of miRNA functions. As the most recently discovered group of noncoding ceRNAs, circRNAs have emerged as potent endogenous sponges. These transcripts are primarily derived from noncanonical head-to-tail splicing events in which a splice donor of an exon backsplices with an upstream splice acceptor from either the same or an upstream exon.[16] The unique circular conformation endows circRNAs with important features for miRNA sequestration.[9,10] It was reported that the general stability of circRNAs is higher than linear transcripts, and circles were shown to be at least 10-fold more resistant to exonucleolytic RNA degradation than linear RNA.[9,10] Furthermore, circRNAs are resistant to miRNA-mediated noncleavage destabilization, but they are susceptible to miRNA-mediated cleavage.[19] In this study, we develop a user-friendly system to express circular miRNA inhibitors, and we demonstrate that the circular miRNA inhibitors are more stable and potent in antagonizing miRNA functions than the linear counterparts.

In addition to circRNA inhibitors, "Tough Decoy" inhibitors (or TuD inhibitors) have been developed as a new sub-class of inhibitors with a special secondary RNA structure, which exhibits the increased overall stability and the accessibility of the miRNA target sites.[9,10] Typical TuD inhibitors contain two opposing target sites at the center of a hairpin-shaped secondary structure, and the double-stranded nature at the termini confers resistance to cellular RNases.[9,10] Another

advantage of the TuD inhibitor system is that to express a multiplexed inhibitor from a single expression cassette ensures synchronized inhibition of several miRNAs, which should have experimental and therapeutic potential for coordinated and parallel suppression of distinct miRNAs, as well as an entire miRNA family. It is conceivable that the TuD design can be introduced into our CimiR vector system.

It is noteworthy that, dependent on its ultimate utility, the CimiR expression module can be subcloned into other viral gene delivery systems, such as adenoviral vector, lentiviral vector, herpes simplex virus (HSV) vector, and adeno-associated virus (AAV) vector, and non-viral gene delivery systems, including *piggyBac* and Sleeping Beauty transposon systems. Thus, these vector systems should significantly diversify the utilities of the CimiR expression as research tools and/or potential therapeutics. Furthermore, the reported CimiR system can be engineered into such a system that one circularized RNA molecule targets multiple miRNAs. Such a feature is important as a given gene is usually modulated by multiple miRNAs.

In summary, we developed and characterized a user-friendly circular miRNA inhibitor expression system, CimiR, which takes advantage of the noncanonical head-to-tail backsplicing mechanism. The splicing sites are brought to a close proximity by two 100-bp IR sequences. In our proof-of-principle experiments, we demonstrate that the circular forms of the miR223-binding site of ARRB1 3′ UTR sponge RNA, bulged anti-miR223 and bulged anti-miR21, exhibit more potent suppression of miRNA activities than their linear counterparts. Thus, the CimiR expression system should be a valuable tool to target miRNAs for basic and translational research.

MATERIALS AND METHODS

Cell Culture and Chemicals

HEK293T, human breast cancer cell lines SKBR3 and MCF7, and human T-ALL cell lines Jurkat and CCRF-CEM were obtained from American Type Culture Collection (ATCC, Manassas, VA). The T-ALL cell lines were maintained in RPMI-1640 with 10% fetal bovine serum (Invitrogen/Thermo Fisher Scientific, Waltham, MA), L-glutamine, and penicillin and streptomycin, while the breast cancer cell lines and 293T cells were maintained in complete DMEM as described.[32–35] For inhibiting the RNA transcription, cells were cultured in the complete medium with 2 nM actinomycin D (Santa Cruz Biotechnology, Dallas, TX) for the indicated times. Unless indicated otherwise, all reagents were purchased from Sigma-Aldrich (St. Louis, MO) or Thermo Fisher Scientific (Waltham, MA).

Construction of Circular and Linear RNA Expression Vectors pSEBR-CimiR, pSEBR-cirBUTR, pSEBR-linBUTR, pSEBR-cirBulg223, and pSEBR-linBulg223

To engineer the IRs in the circRNA expression vectors, we PCR amplified a 100-bp fragment from mouse Rosa26 genomic sequence. The IR sequence is followed by the RNA-splicing branch site, polypyrimidine track, and linker sites for cloning anti-miR sequences (Figures 1A and 1B), and this was cloned into our homemade retroviral vector pSEBR-FLAG at the BglII and *Mlu* I sites. The 100-bp IR was then cloned in the inverse orientation into this vector by adding the splicing donor site of intron and a 20-bp random sequence at its 5′ end (Figures 1A and 1B). The resultant vector was designated as pSEBR-CimiR, which also co-expresses monomeric RFP as a tracking marker. In this vector, the expression of the sequence between the IR sequences is driven by the previously well-characterized constitutive hEFH promoter.[21,22] A control vector only expressing linear RNA, pSEBR-LimiR, was also constructed in a similar fashion except that it lacked the 5′ end IR fragment, the RNA-splicing branch site, and the polypyrimidine track (Figure 1A).

To express a miRNA sponge in a circular form, we PCR amplified and cloned a 402-bp fragment surrounding the hsa-miR223-binding site of the 3′ UTR region (or BUTR) of ARRB1 into pSEBR-CimiR, resulting in pSEBR-cirBUTR. The same BUTR fragment was cloned into pSEBR-LimiR and yielded pSEBR-linBUTR vector. Similarly, we subcloned tandem bulge-containing antagonist sequences of hsa-miR223 and hsa-miR21 into pSEBR-CimiR and pSEBR-LimiR, and we generated pSEBR-cirBulg223, pSEBR-cirBulg21, pSEBR-linBulg223, and pSEBR-linBulg21 retroviral vectors. All PCR-amplified sequences and oligo cassette-cloning constructs were verified by DNA sequencing. Detailed vector construction information is available upon request.

Construction of miRNA Expression Vector for hsa-miR223

To overexpress hsa-miR223, we PCR amplified a human genomic DNA fragment containing miR223 transcript sequence plus 200-bp upstream and downstream sequences, and we subcloned into a retroviral vector pSEB, resulting in pSEB-hsa-miR223. The PCR-amplified sequence was verified by DNA sequencing.

Construction of BUTR Reporter and Gaussia Luciferase Assay

To construct BUTR-GLuc reporter, we PCR amplified and cloned a 402-bp fragment surrounding the hsa-miR223-binding site of the 3′ UTR region (or BUTR) of ARRB1 into our homemade miRNA reporter vector pNRGLuc, as previously reported,[36] and this process yielded pNRGLuc-BUTR.

For the Gaussia luciferase reporter assay, the miR223 overexpression HEK293 cells (293-miR223) were plated in 12-well cell culture plates at 60% confluence, and they were co-transfected with pNRGLuc-BUTR and pSEBR-cirBulg223, pSEBR-linBulg223, empty vector (blank), or the seed sequence SCR expression control vector. The culture medium was used for Gaussian luciferase assay every 24 hr using the BioLux Gaussia Luciferase Assay Kit (New England Biolabs, Ipswich, MA), as previously described.[37–39]

RNA Isolation and Touchdown qPCR Analysis

Total RNA was extracted by using the NucleoZOL Reagent according to the manufacturer's instructions (Takara Bio USA, Mountain View, CA). To synthesize the cDNA for mRNA or mature miRNA quantification, random hexamer, the miRNAs' specific stem-loop primers, and the reverse primer of Gapdh were incubated together with total RNA at 70°C for 5 min and then reverse transcribed with

M-MuLV Reverse Transcriptase (New England Biolabs). The resultant cDNA products were diluted 10- to 50-fold and used as templates for touchdown qPCR (TqPCR). PCR primers were designed by Primer3 Plus program (Table S1). The TqPCR analysis was carried out with our optimized TqPCR protocol[40] using the 2× SYBR Green qPCR master mix (Bimake, Houston, TX). A typical TqPCR program was as follows:[40] 95°C × 3 s for one cycle; 95°C × 20 s, 66°C × 10 s, for 4 cycles by decreasing 3°C per cycle; and 95°C × 20 s, 55°C × 10 s, 70°C × 1 s, followed by plate read, for 40 cycles. Each assay condition was performed in triplicate. All sample values were normalized to Gapdh expression by using the $2^{-\Delta\Delta Ct}$ method as described.[41–43]

Immunofluorescence Staining

Immunofluorescence staining was performed as described.[34,41,44–46] Experimentally, cells were fixed with 4% paraformaldehyde for 15 min. After washing with PBS 3 times, the cells were permeabilized with 1% NP-40 and blocked 10% donkey serum (Jackson ImmunoResearch Laboratories, West Grove, PA, USA), followed by incubating with the the anti-cleaved caspase-3 (Cell Signaling Technology, USA) for 2 hr at room temperature.[34,44,45] After being washed, cells were incubated with fluorescein isothiocyanate (FITC)-labeled anti-mouse immunoglobulin G (IgG) secondary antibody (Jackson ImmunoResearch Laboratories, West Grove, PA) for 30 min. The cell nuclei were counterstained with DAPI. Stains without primary antibodies were used as negative controls. Fluorescence images were recorded under an inverted fluorescence microscope.

Cell Cycle Analysis

Exponentially growing cells were infected with the respective retroviral vectors. The cells were harvested at the indicated time points, fixed, stained with Hoechst 33258, and subjected to fluorescence-activated cell sorting (FACS) analysis as described.[47,48]

Colony Formation Assay

Human breast cancer cells were infected with retroviral vectors for 36 hr, and then they were plated in 60-mm^2 cell culture dishes with two initial cell numbers in triplicate, as previously reported.[49,50] After 12 days, cell colonies were stained with crystal violet and recorded macrographically. The numbers of colonies were counted for quantitative analysis.

Western Blotting Assay

Cells were lyzed in 2× Laemmli buffer and subjected to SDS-PAGE, followed by transferrence to a polyvinylidene fluoride (PVDF) membrane and blotting with anti-GAPDH (Proteintech Group, Rosemont, IL), anti-BCL2 (Santa Cruz Biotechnology), and anti-PTEN (Santa Cruz Biotechnology) antibodies. The presence of the proteins of interest was visualized by enhanced chemiluminescence as described.[46,51–54]

Xenograft Tumor Formation and Optical Imaging

The use and care of animals was approved by the Institutional Animal Care and Use Committee of The University of Chicago (IACUC Protocol 71328). All animal experiments were performed in accordance with the guidelines and regulations stipulated in the approved protocol. Experimentally, the SKBR3 cells stably expressing firefly luciferase were infected with retroviral vectors expressing linBulg21, cirBulg21, or seed sequence SCR control. At 48 hr after infection, 5×10^6 cells per site were injected subcutaneously into nude mice at the indicated positions (n = 5 mice, female, 6–8 weeks old, Harlan Laboratories). The animals were subjected to imaging with Xenogen IVIS 200 system (Xenogen, Alameda, CA, USA) at the indicated time points. Briefly, mice were injected (intraperitoneally [i.p.]) with D-Luciferin sodium salt (Gold Biotechnology, St. Louis, MO) at 100 mg/kg in 0.1 mL PBS. The pseudo-images were obtained by superimposing the emitted light over the gray-scale photographs of the mice. Quantitative analysis was conducted with Xenogen's Living Image software as described.[55–57] At 26 days after transplantation, the mice were euthanized and the tumor masses were collected for histologic evaluation.

H&E Staining

H&E staining was done as described.[37,39,58] Briefly, the retrieved specimens were fixed with 10% formalin, decalcified, and embedded in paraffin. Serial sections at 5 μm of the embedded specimens were deparaffinized and subjected to H&E staining as described.[37,39,58]

Statistical Analysis

All quantitative experiments were performed in triplicate and/or repeated in three independent batches of experiments. Data were expressed as mean ± SD. The one-way ANOVA was used to analyze statistical significance.[38] A value of $p < 0.05$ was considered statistically significant.

SUPPLEMENTAL INFORMATION

Supplemental Information includes one figure and one table and can be found with this article online at https://doi.org/10.1016/j.omtn.2018.09.025.

AUTHOR CONTRIBUTIONS

Y. Shu, K.W., and T.-C.H. conceived and designed the study. Y. Shu, Z.Z., S.H., X.J., and L. Zhang performed the experiments and collected data. W. Liu, B.H., Y.F., B.Z., Z.D., Y. Shen, W. Luo, X.W., B.L., Y.L., Z.Y., L. Zhao, D.C., L.Y., and X.C. participated in molecular cloning experiments; provided essential experimental materials; and assisted in histological preparations, immunostaining, and qPCR data analysis and interpretations. Y. Shu, T.-C.H., H.H.L., R.R.R., J.M.W., M.J.L., and K.W. drafted and revised the manuscript. All authors reviewed and approved the manuscript.

CONFLICTS OF INTEREST

The authors have no conflicts of interest.

ACKNOWLEDGMENTS

The reported work was supported in part by research grants from the NIH (CA226303 and DE020140 to T.-C.H. and R.R.R.), the U.S. Department of Defense (OR130096 to J.M.W.), the Chicago Biomedical Consortium with support from the Searle Funds at The Chicago

Community Trust (R.R.R. and T.-C.H.), the Scoliosis Research Society (T.-C.H. and M.J.L.), and the National Key Research and Development Program of China (2016YFC1000803 and 2011CB707906 to T.-C.H.). Y. Shu, Z.Z., B.H., Y.F., and B.Z. were recipients of the pre-doctorate fellowship from the China Scholarship Council. This project was also supported in part by The University of Chicago Cancer Center Support Grant (P30CA014599) and the National Center for Advancing Translational Sciences of the NIH through grant UL1 TR000430. T.-C.H. was also supported by the Mabel Green Myers Research Endowment Fund and The University of Chicago Orthopaedic Surgery Alumni Fund. Funding sources were not involved in the study design; the collection, analysis, and interpretation of data; the writing of the report; and the decision to submit the paper for publication.

REFERENCES

1. He, L., and Hannon, G.J. (2004). MicroRNAs: small RNAs with a big role in gene regulation. Nat. Rev. Genet. *5*, 522–531.
2. Lagos-Quintana, M., Rauhut, R., Lendeckel, W., and Tuschl, T. (2001). Identification of novel genes coding for small expressed RNAs. Science *294*, 853–858.
3. Bartel, D.P. (2004). MicroRNAs: genomics, biogenesis, mechanism, and function. Cell *116*, 281–297.
4. Rupaimoole, R., and Slack, F.J. (2017). MicroRNA therapeutics: towards a new era for the management of cancer and other diseases. Nat. Rev. Drug Discov. *16*, 203–222.
5. Bartel, D.P. (2009). MicroRNAs: target recognition and regulatory functions. Cell *136*, 215–233.
6. Friedman, R.C., Farh, K.K., Burge, C.B., and Bartel, D.P. (2009). Most mammalian mRNAs are conserved targets of microRNAs. Genome Res. *19*, 92–105.
7. Di Leva, G., Garofalo, M., and Croce, C.M. (2014). MicroRNAs in cancer. Annu. Rev. Pathol. *9*, 287–314.
8. Gurha, P. (2016). MicroRNAs in cardiovascular disease. Curr. Opin. Cardiol. *31*, 249–254.
9. Bak, R.O., Hollensen, A.K., and Mikkelsen, J.G. (2013). Managing microRNAs with vector-encoded decoy-type inhibitors. Mol. Ther. *21*, 1478–1485.
10. Bak, R.O., and Mikkelsen, J.G. (2014). miRNA sponges: soaking up miRNAs for regulation of gene expression. Wiley Interdiscip. Rev. RNA *5*, 317–333.
11. van Rooij, E., and Olson, E.N. (2012). MicroRNA therapeutics for cardiovascular disease: opportunities and obstacles. Nat. Rev. Drug Discov. *11*, 860–872.
12. van Rooij, E., and Kauppinen, S. (2014). Development of microRNA therapeutics is coming of age. EMBO Mol. Med. *6*, 851–864.
13. Zhang, X.O., Wang, H.B., Zhang, Y., Lu, X., Chen, L.L., and Yang, L. (2014). Complementary sequence-mediated exon circularization. Cell *159*, 134–147.
14. Cocquerelle, C., Daubersies, P., Majérus, M.A., Kerckaert, J.P., and Bailleul, B. (1992). Splicing with inverted order of exons occurs proximal to large introns. EMBO J. *11*, 1095–1098.
15. Cocquerelle, C., Mascrez, B., Hétuin, D., and Bailleul, B. (1993). Mis-splicing yields circular RNA molecules. FASEB J. *7*, 155–160.
16. Jeck, W.R., Sorrentino, J.A., Wang, K., Slevin, M.K., Burd, C.E., Liu, J., Marzluff, W.F., and Sharpless, N.E. (2013). Circular RNAs are abundant, conserved, and associated with ALU repeats. RNA *19*, 141–157.
17. Salzman, J., Gawad, C., Wang, P.L., Lacayo, N., and Brown, P.O. (2012). Circular RNAs are the predominant transcript isoform from hundreds of human genes in diverse cell types. PLoS ONE *7*, e30733.
18. Ashwal-Fluss, R., Meyer, M., Pamudurti, N.R., Ivanov, A., Bartok, O., Hanan, M., Evantal, N., Memczak, S., Rajewsky, N., and Kadener, S. (2014). circRNA biogenesis competes with pre-mRNA splicing. Mol. Cell *56*, 55–66.
19. Hansen, T.B., Jensen, T.I., Clausen, B.H., Bramsen, J.B., Finsen, B., Damgaard, C.K., and Kjems, J. (2013). Natural RNA circles function as efficient microRNA sponges. Nature *495*, 384–388.
20. Dubin, R.A., Kazmi, M.A., and Ostrer, H. (1995). Inverted repeats are necessary for circularization of the mouse testis Sry transcript. Gene *167*, 245–248.
21. Wen, S., Zhang, H., Li, Y., Wang, N., Zhang, W., Yang, K., Wu, N., Chen, X., Deng, F., Liao, Z., et al. (2014). Characterization of constitutive promoters for piggyBac transposon-mediated stable transgene expression in mesenchymal stem cells (MSCs). PLoS ONE *9*, e94397.
22. Luo, Q., Kang, Q., Song, W.X., Luu, H.H., Luo, X., An, N., Luo, J., Deng, Z.L., Jiang, W., Yin, H., et al. (2007). Selection and validation of optimal siRNA target sites for RNAi-mediated gene silencing. Gene *395*, 160–169.
23. Ebert, M.S., Neilson, J.R., and Sharp, P.A. (2007). MicroRNA sponges: competitive inhibitors of small RNAs in mammalian cells. Nat. Methods *4*, 721–726.
24. Ebert, M.S., and Sharp, P.A. (2010). MicroRNA sponges: progress and possibilities. RNA *16*, 2043–2050.
25. Acunzo, M., Romano, G., Nigita, G., Veneziano, D., Fattore, L., Laganà, A., Zanesi, N., Fadda, P., Fassan, M., Rizzotto, L., et al. (2017). Selective targeting of point-mutated KRAS through artificial microRNAs. Proc. Natl. Acad. Sci. USA *114*, E4203–E4212.
26. Mavrakis, K.J., Van Der Meulen, J., Wolfe, A.L., Liu, X., Mets, E., Taghon, T., Khan, A.A., Setty, M., Rondou, P., Vandenberghe, P., et al. (2011). A cooperative microRNA-tumor suppressor gene network in acute T-cell lymphoblastic leukemia (T-ALL). Nat. Genet. *43*, 673–678.
27. Mansour, M.R., Sanda, T., Lawton, L.N., Li, X., Kreslavsky, T., Novina, C.D., Brand, M., Gutierrez, A., Kelliher, M.A., Jamieson, C.H., et al. (2013). The TAL1 complex targets the FBXW7 tumor suppressor by activating miR-223 in human T cell acute lymphoblastic leukemia. J. Exp. Med. *210*, 1545–1557.
28. Frankel, L.B., Christoffersen, N.R., Jacobsen, A., Lindow, M., Krogh, A., and Lund, A.H. (2008). Programmed cell death 4 (PDCD4) is an important functional target of the microRNA miR-21 in breast cancer cells. J. Biol. Chem. *283*, 1026–1033.
29. Park, C.Y., Choi, Y.S., and McManus, M.T. (2010). Analysis of microRNA knockouts in mice. Hum. Mol. Genet. *19* (R2), R169–R175.
30. Prosser, H.M., Koike-Yusa, H., Cooper, J.D., Law, F.C., and Bradley, A. (2011). A resource of vectors and ES cells for targeted deletion of microRNAs in mice. Nat. Biotechnol. *29*, 840–845.
31. Gentner, B., Schira, G., Giustacchini, A., Amendola, M., Brown, B.D., Ponzoni, M., and Naldini, L. (2009). Stable knockdown of microRNA in vivo by lentiviral vectors. Nat. Methods *6*, 63–66.
32. Zhu, G.H., Huang, J., Bi, Y., Su, Y., Tang, Y., He, B.C., He, Y., Luo, J., Wang, Y., Chen, L., et al. (2009). Activation of RXR and RAR signaling promotes myogenic differentiation of myoblastic C2C12 cells. Differentiation *78*, 195–204.
33. Huang, J., Bi, Y., Zhu, G.H., He, Y., Su, Y., He, B.C., Wang, Y., Kang, Q., Chen, L., Zuo, G.W., et al. (2009). Retinoic acid signalling induces the differentiation of mouse fetal liver-derived hepatic progenitor cells. Liver Int. *29*, 1569–1581.
34. Huang, E., Bi, Y., Jiang, W., Luo, X., Yang, K., Gao, J.L., Gao, Y., Luo, Q., Shi, Q., Kim, S.H., et al. (2012). Conditionally immortalized mouse embryonic fibroblasts retain proliferative activity without compromising multipotent differentiation potential. PLoS ONE *7*, e32428.
35. Huang, E., Zhu, G., Jiang, W., Yang, K., Gao, Y., Luo, Q., Gao, J.L., Kim, S.H., Liu, X., Li, M., et al. (2012). Growth hormone synergizes with BMP9 in osteogenic differentiation by activating the JAK/STAT/IGF1 pathway in murine multilineage cells. J. Bone Miner. Res. *27*, 1566–1575.
36. Liao, J., Yu, X., Hu, X., Fan, J., Wang, J., Zhang, Z., Zhao, C., Zeng, Z., Shu, Y., Zhang, R., et al. (2017). lncRNA H19 mediates BMP9-induced osteogenic differentiation of mesenchymal stem cells (MSCs) through Notch signaling. Oncotarget *8*, 53581–53601.
37. Ye, J., Wang, J., Zhu, Y., Wei, Q., Wang, X., Yang, J., Tang, S., Liu, H., Fan, J., Zhang, F., et al. (2016). A thermoresponsive polydiolcitrate-gelatin scaffold and delivery system mediates effective bone formation from BMP9-transduced mesenchymal stem cells. Biomed. Mater. *11*, 025021.
38. Zhang, F., Li, Y., Zhang, H., Huang, E., Gao, L., Luo, W., Wei, Q., Fan, J., Song, D., Liao, J., et al. (2017). Anthelmintic mebendazole enhances cisplatin's effect on

suppressing cell proliferation and promotes differentiation of head and neck squamous cell carcinoma (HNSCC). Oncotarget *8*, 12968–12982.

39. Zhang, H., Wang, J., Deng, F., Huang, E., Yan, Z., Wang, Z., Deng, Y., Zhang, Q., Zhang, Z., Ye, J., et al. (2015). Canonical Wnt signaling acts synergistically on BMP9-induced osteo/odontoblastic differentiation of stem cells of dental apical papilla (SCAPs). Biomaterials *39*, 145–154.

40. Zhang, Q., Wang, J., Deng, F., Yan, Z., Xia, Y., Wang, Z., Ye, J., Deng, Y., Zhang, Z., Qiao, M., et al. (2015). TqPCR: A Touchdown qPCR Assay with Significantly Improved Detection Sensitivity and Amplification Efficiency of SYBR Green qPCR. PLoS ONE *10*, e0132666.

41. Hu, X., Li, L., Yu, X., Zhang, R., Yan, S., Zeng, Z., Shu, Y., Zhao, C., Wu, X., Lei, J., et al. (2017). CRISPR/Cas9-mediated reversibly immortalized mouse bone marrow stromal stem cells (BMSCs) retain multipotent features of mesenchymal stem cells (MSCs). Oncotarget *8*, 111847–111865.

42. Wei, Q., Fan, J., Liao, J., Zou, Y., Song, D., Liu, J., Cui, J., Liu, F., Ma, C., Hu, X., et al. (2017). Engineering the Rapid Adenovirus Production and Amplification (RAPA) Cell Line to Expedite the Generation of Recombinant Adenoviruses. Cell. Physiol. Biochem. *41*, 2383–2398.

43. Liao, J., Wei, Q., Fan, J., Zou, Y., Song, D., Liu, J., Liu, F., Ma, C., Hu, X., Li, L., et al. (2017). Characterization of retroviral infectivity and superinfection resistance during retrovirus-mediated transduction of mammalian cells. Gene Ther. *24*, 333–341.

44. Wang, N., Zhang, H., Zhang, B.Q., Liu, W., Zhang, Z., Qiao, M., Zhang, H., Deng, F., Wu, N., Chen, X., et al. (2014). Adenovirus-mediated efficient gene transfer into cultured three-dimensional organoids. PLoS ONE *9*, e93608.

45. Wang, N., Zhang, W., Cui, J., Zhang, H., Chen, X., Li, R., Wu, N., Chen, X., Wen, S., Zhang, J., et al. (2014). The piggyBac transposon-mediated expression of SV40 T antigen efficiently immortalizes mouse embryonic fibroblasts (MEFs). PLoS ONE *9*, e97316.

46. Kong, Y., Zhang, H., Chen, X., Zhang, W., Zhao, C., Wang, N., Wu, N., He, Y., Nan, G., Zhang, H., et al. (2013). Destabilization of heterologous proteins mediated by the GSK3β phosphorylation domain of the β-catenin protein. Cell. Physiol. Biochem. *32*, 1187–1199.

47. Deng, Y., Wang, Z., Zhang, F., Qiao, M., Yan, Z., Wei, Q., Wang, J., Liu, H., Fan, J., Zou, Y., et al. (2016). A Blockade of IGF Signaling Sensitizes Human Ovarian Cancer Cells to the Anthelmintic Niclosamide-Induced Anti-Proliferative and Anticancer Activities. Cell. Physiol. Biochem. *39*, 871–888.

48. Deng, Y., Zhang, J., Wang, Z., Yan, Z., Qiao, M., Ye, J., Wei, Q., Wang, J., Wang, X., Zhao, L., et al. (2015). Antibiotic monensin synergizes with EGFR inhibitors and oxaliplatin to suppress the proliferation of human ovarian cancer cells. Sci. Rep. *5*, 17523.

49. Luu, H.H., Kang, Q., Park, J.K., Si, W., Luo, Q., Jiang, W., Yin, H., Montag, A.G., Simon, M.A., Peabody, T.D., et al. (2005). An orthotopic model of human osteosarcoma growth and spontaneous pulmonary metastasis. Clin. Exp. Metastasis *22*, 319–329.

50. Haydon, R.C., Zhou, L., Feng, T., Breyer, B., Cheng, H., Jiang, W., Ishikawa, A., Peabody, T., Montag, A., Simon, M.A., and He, T.C. (2002). Nuclear receptor agonists as potential differentiation therapy agents for human osteosarcoma. Clin. Cancer Res. *8*, 1288–1294.

51. Peng, Y., Kang, Q., Luo, Q., Jiang, W., Si, W., Liu, B.A., Luu, H.H., Park, J.K., Li, X., Luo, J., et al. (2004). Inhibitor of DNA binding/differentiation helix-loop-helix proteins mediate bone morphogenetic protein-induced osteoblast differentiation of mesenchymal stem cells. J. Biol. Chem. *279*, 32941–32949.

52. Si, W., Kang, Q., Luu, H.H., Park, J.K., Luo, Q., Song, W.X., Jiang, W., Luo, X., Li, X., Yin, H., et al. (2006). CCN1/Cyr61 is regulated by the canonical Wnt signal and plays an important role in Wnt3A-induced osteoblast differentiation of mesenchymal stem cells. Mol. Cell. Biol. *26*, 2955–2964.

53. Paul, R., Haydon, R.C., Cheng, H., Ishikawa, A., Nenadovich, N., Jiang, W., Zhou, L., Breyer, B., Feng, T., Gupta, P., et al. (2003). Potential use of Sox9 gene therapy for intervertebral degenerative disc disease. Spine *28*, 755–763.

54. Su, Y.A., Lee, M.M., Hutter, C.M., and Meltzer, P.S. (1997). Characterization of a highly conserved gene (OS4) amplified with CDK4 in human sarcomas. Oncogene *15*, 1289–1294.

55. Luo, X., Chen, J., Song, W.X., Tang, N., Luo, J., Deng, Z.L., Sharff, K.A., He, G., Bi, Y., He, B.C., et al. (2008). Osteogenic BMPs promote tumor growth of human osteosarcomas that harbor differentiation defects. Lab. Invest. *88*, 1264–1277.

56. Liao, Z., Nan, G., Yan, Z., Zeng, L., Deng, Y., Ye, J., Zhang, Z., Qiao, M., Li, R., Denduluri, S., et al. (2015). The Anthelmintic Drug Niclosamide Inhibits the Proliferative Activity of Human Osteosarcoma Cells by Targeting Multiple Signal Pathways. Curr. Cancer Drug Targets *15*, 726–738.

57. Li, R., Zhang, W., Cui, J., Shui, W., Yin, L., Wang, Y., Zhang, H., Wang, N., Wu, N., Nan, G., et al. (2014). Targeting BMP9-promoted human osteosarcoma growth by inactivation of notch signaling. Curr. Cancer Drug Targets *14*, 274–285.

58. Wang, J., Zhang, H., Zhang, W., Huang, E., Wang, N., Wu, N., Wen, S., Chen, X., Liao, Z., Deng, F., et al. (2014). Bone morphogenetic protein-9 effectively induces osteo/odontoblastic differentiation of the reversibly immortalized stem cells of dental apical papilla. Stem Cells Dev. *23*, 1405–1416.